Journal of Power Sources 218 (2012) 297–306

Contents lists available at SciVerse ScienceDirect

Journal of Power Sources

journal homepage: www.elsevier.com/locate/jpowsour

Exploring the potential of exfoliated graphene nanoplatelets as the conductive filler in polymeric nanocomposites for bipolar plates

Xian Jiang*, Lawrence T. Drzal

Michigan State University, Composite Materials and Structures Center, Department of Chemical Engineering and Materials Science, East Lansing, MI 48824, USA

HIGHLIGHTS

- ► An easy but effective compounding method (SSBM) was used to fabricate bipolar plates.
- ► Synergistic effects between GNP, carbon black and GNP of different sizes were investigated.
- ► Highly conductive PPS impregnated GNP papers were fabricated.
- ► PPS impregnated GNP papers were embedded into bipolar plates to improve various properties.

ARTICLE INFO

Article history:
Received 28 March 2012
Received in revised form
29 June 2012
Accepted 1 July 2012
Available online 7 July 2012

Keywords:
Exfoliated graphene nanoplatelets
Nanocomposites
Bipolar plates
Electrical conductivity
Mechanical properties

ABSTRACT

This research explored the potential of using exfoliated graphene nanoplatelets, GNP, as the conductive filler to construct highly conductive polymeric nanocomposites to substitute for conventional metallic and graphite bipolar plates in the polymer electrolyte membrane (PEM) fuel cells. Polyphenylene sulfide (PPS) was selected as the polymer matrix because of its high thermal and chemical tolerance. Solid state ball milling (SSBM) followed by compression molding was then applied to fabricate PPS/GNP nanocomposites. Results showed that PPS/GNP nanocomposites made by this method exhibit excellent mechanical and gas barrier properties but unsatisfied electrical conductivity. However, it was found that the electrical conductivity of these nanocomposites could be substantially enhanced if we combine GNP with second minor conductive filler for a positive synergistic effect and also optimize the processing time of SSBM. Meanwhile, PPS impregnated GNP papers were embedded into these PPS/GNP nanocomposites in order to further improve various properties of the resulting bipolar plates. It is believed that the bipolar plates made from PPS/GNP nanocomposites will allow lighter weight of PEM fuel cells with enhanced performance which is particularly suited for automotive applications.

1. Introduction

PEM fuel cell is a relatively new but fast developing power system which is considered to be one of the most promising power sources for stationary and transportation application in the future due to its high efficiency, high-power density, convenient fuel supply, and long-life time [1,2]. Fuel cells produce electrical energy by converting the chemical energy stored in certain fuels like hydrogen and methanol through oxidation and reduction reactions [3]. A key component in fuel cells is bipolar plates which account for approximately 80% of the fuel cell volume, 70% of the fuel cell weight and as much as 60% of the entire stack cost [4]. The importance of bipolar plates in fuel cells is fully reflected by these major functions they serve: such as providing a uniform distribution of fuel gas and oxygen within the cell, facilitating water management, conducting electrical current from one single fuel cell to another, enabling heat transfer, and providing adequate mechanical strength to resist the clamping forces for the fuel cell stack assembly [5]. To meet all these functions, bipolar plates must exhibit excellent electrical and thermal conductivity, adequate mechanical strength, good chemical corrosion resistance, and low gas permeability [6,7]. Moreover, good processability and low manufacturing cost are generally required if bipolar plates are to be widely used in industry [8,9].

Traditionally, bipolar plates are made from metallic materials and graphite [4,10]. Metallic materials such as steel and copper have the attributes of excellent electrical and thermal conductivity, good mechanical strength, low cost, and ease to fabricate. But their oxidation and chemical corrosion resistance under the fuel cell operation atmosphere is really poor [11]. In this case, additional coatings are needed on the surface of these metallic bipolar plates

* Corresponding author. Tel.: +1 517 353 4708; fax: +1 517 432 1634.
E-mail address: jiangxi3@msu.edu (X. Jiang).

0378-7753/$ – see front matter © 2012 Elsevier B.V. All rights reserved.
http://dx.doi.org/10.1016/j.jpowsour.2012.07.001

for corrosion protection [12,13]. However, due to the different thermal expansion coefficient between the coating layer and the metal plate, micro-pores and micro-cracks are normally formed after certain time of fuel cell operation, which eventually deteriorate the protection from the coatings and even cause extra ohmic losses [3]. Bipolar plates made from graphite have the advantages of high oxidation and chemical corrosion resistance, good electrical and thermal conductivity. But due to its brittleness, it is very difficult to carve gas channels on the surface [14], which makes the manufacturing cost very high and limits the utilization of graphite bipolar plates for real applications.

These drawbacks of conventional materials have motivated researchers to develop alternative products for bipolar plates. A composite bipolar plate is then considered as a promising alternative to both metal and graphite because it offers the characteristics of lower cost, higher processability and lighter weight. Furthermore, gas flow channels can be easily molded into their surface without a costly secondary machining step [15–17]. However, polymeric composites are associated with the problem of balancing the electrical conductivity with their mechanical strength. In order to meet the DOE requirement of electrical conductivity (>100 S cm^{-1}) [6], excessive conductive fillers should be incorporated, which conversely reduce the mechanical strength and ductility of the composites [18]. Recently, carbon fiber, carbon black, natural or synthetic graphite, and combinations thereof have been extensively explored as the conductive fillers to fabricate polymeric bipolar plates. For these conductive fillers, although their price is low, it was found that the loading should be as high as 70 wt% to achieve an adequate electrical conductivity. At this high filler content, the mechanical strength of the resulting composites is usually poor [19]. In this case, how to achieve a high electrical conductivity while maintaining good mechanical properties in polymeric composites still remains an important research topic to be explored. And the key issue to solve this problem is to carefully select one or more appropriate conductive fillers that could implement excellent electrical conductivity at relatively low filler loadings.

In this research, exfoliated graphene nanoplatelets, GNP, was then chosen as the major conductive filler, which is due to its excellent mechanical and structural properties, superior electrical and thermal conductivity, and extremely low gas permeability as shown in the research work of Dr. Drzal group [20–23]. Carbon black was considered as minor conductive filler to attain a positive synergistic effect with GNP. Polyphenylene sulfide (PPS) was selected as the polymer matrix on the account of its superior chemical corrosion and oxidation resistance, excellent mechanical properties, and high-temperature stability [24]. And the advantages of using thermoplastics as the polymer matrix over thermosets are their attributes of recyclability, higher processability, shorter processing time and potentially lower cost. The compounding method of fabricating PPS/GNP nanocomposites is solid state ball milling (SSBM) followed by compression molding. The reason of selecting this compounding method is because of its capability of achieving a high electrical conductivity in GNP nanocomposites as described in a previous study [25]. In the SSBM process, it was found that polymer particles are uniformly coated with GNP platelets which facilitate the formation of conductive pathways during the following injection molding or compression molding steps. The electrical conductivity of the resulting nanocomposites is thus excellent. It is believed that GNP based PPS nanocomposites made from this compounding technique may offer the potential to satisfy the DOE target for the electrical conductivity while maintaining the GNP content at relatively low levels (≤60 wt %) to ensure a good mechanical strength.

Meanwhile, reassembly of nano-material into macro-scale structures has also become an interesting research object to fully utilize the excellent properties of nano-fillers. CNT paper (Bucky paper) [26–28], CNF paper [29,30], and reduced graphite oxide (RGO) paper [31,32] have been extensively explored for several years. Reassembly of these nano-fillers into the paper form provides the characteristics of light-weight, high mechanical robustness and flexibility, excellent thermal and electrical conductivity to the resulting papers, which are valuable for many applications such as current collector, heat dissipater, lightening protector, armor plating and filter membrane [33,34]. Moreover, these nano-filler papers can be used as matting to be embedded into polymeric composites to enhance their mechanical, thermal and electrical properties. Results showed that the property enhancement by incorporating nano-filler papers is much greater than that from directly mixing the nano-filler with polymers [35]. It is known that nano-reinforcements normally do not disperse well within polymers and they tend to closely stack with each other in forming aggregates, which constrains the translation of superb properties of nano-fillers into the resulting nanocomposites. Therefore, the application of nano-filler papers offers a promising method to fully utilize their excellent properties.

Research work in Drzal group has demonstrated that GNP can also be reassembled into a paper form by applying a vacuum filtration method [35]. GNP papers made by this technique are self-standing, robust and have some mechanical flexibility. It was reported that the in-plane electrical conductivity of a GNP paper is over 1300 S cm^{-1} and its in-plane thermal conductivity is more than 300 W $(mK)^{-1}$. In addition, the gas permeability of a GNP paper is extremely low. GNP papers are thus considered as good components in polymeric nanocomposites to further enhance their various properties for the application in bipolar plates.

2. Experimental

2.1. Materials

In this research, PPS powder with the trade name Fortron® 0205 (powder size: 300–400 μm, density: 1.35 g cm^{-3}) was obtained from Ticona. GNP nanoplatelets with the diameter around 25 and 15 μm (GNP-25 and GNP-15) and thickness around 5–10 nm were from XG Science, Inc [36]. 'High Structure' carbon black (CB, KETJENBLACK EC-600 JD, aggregate size: 30–100 nm) was from AkzoNobel Polymer Chemicals LLC. Polyethylenimine (branched, PEI) from Sigma–Aldrich was used to help the dispersion of PPS and GNP in water.

2.2. Solid state ball milling (SSBM) and compression molding

The starting material for SSBM is a mixture of as-received PPS powder and GNP-25 nanoplatelets. SSBM process was carried out in an SPEX SamplePrep 8000D Dual Mixer/Mill® system which is shown in Fig. 1. The mixture of GNP and PPS powder at selected weight ratios (10 wt%, 20 wt%, 30 wt%, 40 wt%, 50 wt%, and 60 wt% GNP loading) was added into a stainless steel vial where six steel balls (2 large balls: 1/4 inch in diameter and 4 small balls: 1/8 inch in diameter) were used as the milling medium. SSBM time was first kept as 200 min and then the SSBM time was adjusted accordingly to optimize the various properties of PPS/GNP nanocomposites which will be fully discussed later. Based on a previous study, SSBM could produce a PPS and GNP powder mixture with PPS particles uniformly coated by GNP platelets [25]. The size of PPS powders and GNP platelets was reduced significantly by the SSBM process. It was found that the final size of PPS was reduced to around 100 μm and the size of GNP-25 was down to less than 5 μm after 200 min ball milling. Then the powder mixture was compression molded into flexural coupons for mechanical and electrical properties test

Fig. 1. SPEX SamplePrep 8000D Dual Mixer/Mill® system and its steel vial set.

and thin films (thickness: ~100 μm) for gas permeability measurement. A lower compression molding temperature of 300 °C was selected to fabricate PPS nanocomposites with less than 40 wt% filler loading for a better processability and a higher temperature of 325 °C was chosen for the nanocomposites containing 40 wt% or higher conductive filler to achieve a better PPS wetting and infiltration. The molding pressure was kept at 25 MPa for all the PPS/GNP nanocomposites.

2.3. Experimental characterization

A UTS SFM-20 machine (United Calibration Corp.) was used to measure the flexural properties. Flexural coupons were tested under 3-point bending mode at a flexural rate of 0.05 in min^{-1} by following the ASTM D790 standard.

Electrical conductivity measurements were taken on the flexural coupons by a four point method. The set-up of the four-point measurement is schematically shown in Fig. 2. For this technique, a current source forces a constant current through the sample bar, which is measured by a separate ammeter. And a voltmeter simultaneously measures the voltage produced across the inner part of the flexural coupon.

The four-point electrical conductivity is then calculated as:

$$\rho = \frac{Vwt}{Il} \qquad S = 1/\rho \tag{1}$$

where ρ = Electrical resistivity of the sample (Ω cm), S = Electrical conductivity of the sample (S cm^{-1}), V = Voltage measured by the voltmeter (V), I = Current measured by the ammeter (A), w = The width of the sample (cm), t = The thickness of the sample (cm), l = The distance between the two points where the voltmeter measures the voltage (cm).

The gas (oxygen) permeability of GNP nanocomposite films was measured based on the ASTM D3985 standard by using a MOCON® Ox-Tran 2/20 instrument at room temperature. The testing pressure was set as 0.21 MPa and the thickness of the composite films was kept at 0.1 mm.

An environmental scanning electron microscopy (ESEM Carl Zeiss EVO) was used to collect the SEM images at an accelerating voltage of 15 kV. Samples were gold coated to avoid charging.

3. Results and discussion

3.1. Various properties of PPS/GNP nanocomposites made by SSBM and compression molding

The flexural properties of PPS/GNP nanocomposites made by SSBM and compression molding are shown in Fig. 3. From this figure, it is noted that the modulus of these nanocomposites exhibits a monotonic increase with the increasing GNP content. At 60 wt% GNP loading, the modulus is enhanced by almost 200% compared to that of neat PPS. Meanwhile, the flexural strength of these PPS/GNP nanocomposites is found to be much lower than the neat PPS but it is not affected much by the increase of GNP content. Especially at 60 wt% GNP loading, the flexural strength of the nanocomposite is still as high as 66 MPa, which is more than twice as much as the DOE requirement for bipolar plates (>25 MPa).

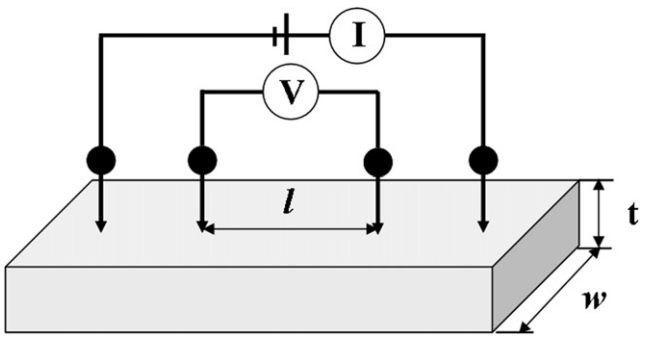

Fig. 2. A four-point technique for measuring the electrical conductivity of GNP nanocomposites.

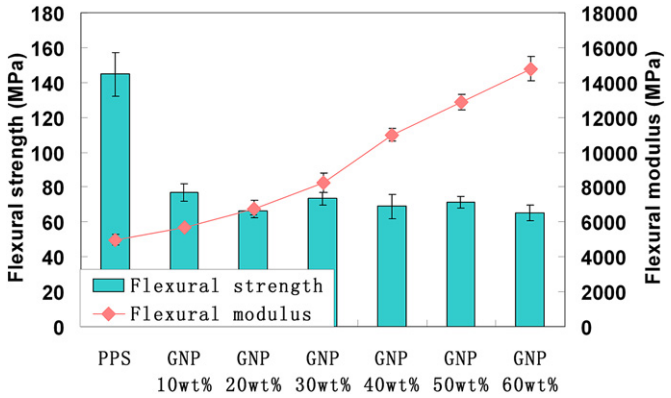

Fig. 3. Flexural properties of PPS/GNP nanocomposites made by SSBM and compression molding.

To have a better understanding for the flexural behavior of these nanocomposites, their strain values at break during the mechanical testing are presented in Fig. 4. According to this figure, a huge decrease in strain at break is observed between the neat PPS and the PPS/GNP sample with 10 wt% GNP, which implies that incorporation of GNP platelets makes PPS much more brittle and less ductile. As the GNP content increases, the strain value at break gradually decreases while the flexural modulus of these nanocomposites increases significantly as shown in Fig. 3. In consequence, the flexural strength stays slightly unchanged.

Fig. 5 describes the gas (Oxygen) permeability of PPS/GNP nanocomposites up to 60 wt% GNP loading. It is seen that the gas permeability firstly drops tremendously from the neat PPS to the nanocomposite with 40 wt% GNP loading then it falls into a plateau. Substantially lower gas permeability in PPS/GNP nanocomposites is due to the excellent gas barrier properties of GNP platelets as the nano-reinforcements [23]. And if compared with the DOE target for the gas permeability [37], it is found that even the neat PPS film could successfully satisfy the requirement. And the permeability value of the PPS/GNP nanocomposite with 60 wt% GNP content is more than two orders of magnitude lower than the DOE target, which suggests that PPS/GNP nanocomposites fabricated by the method of SSBM and compression mold can meet the permeability request for bipolar plates.

The in-plane electrical conductivity of these nanocomposites is then displayed in Fig. 6. It is seen that although the electrical conductivity exhibits a dramatic increase with the increasing GNP content, it is still falling short of the DOE target (>100 S cm^{-1}) even at 60 wt% GNP loading, which implies that using GNP alone as the single conductive filler may not be sufficient to provide enough conductive pathways for a desired electrical conductivity. Based on a previous study, micro-pores and micro-gaps are normally present between GNP nanoplatelets, which tremendously inhibit the electron transportation throughout the polymer matrix and thus lower the electrical conductivity in the resulting nanocomposites [38].

3.2. Synergistic effect in PPS/CB/GNP hybrid nanocomposites

In order to enhance the electrical conductivity of PPS/GNP nanocomposites to meet the DOE requirement for bipolar plates, combination of GNP with a second conductive filler of different geometry was considered to fill up the micro-pores and micro-gaps for a positive synergistic effect. In this study, CB was selected for this purpose based on its appropriate size and round shape. The hybridized PPS/CB/GNP nanocomposites were also fabricated by the same SSBM and compression molding process as described in the Experimental section. The total filler loading was kept constant

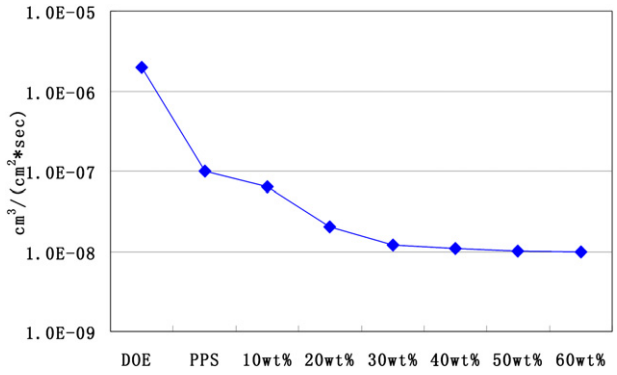

Fig. 5. Gas permeability of PPS/GNP nanocomposites made by SSBM and compression molding.

at 60 wt% and the weight ratio between CB and GNP was changing from 10:50 to 30:30 wt%. The electrical and mechanical properties of these hybridized nanocomposites are shown in Figs. 7 and 8 respectively.

As seen from the electrical measurement in Fig. 7, there is a sharp increase in the electrical conductivity even when 10 wt% GNP is substituted by CB. And as the weight ratio between CB and GNP increases to 1:2, the electrical conductivity goes to a maximum at around 32 S cm^{-1}, which is more than 5 times higher than that of the control sample (PPS/GNP 60 wt%). Significantly enhanced electrical conductivity indicates a positive synergistic effect between GNP platelets and CB particles in facilitating the electron transportation throughout the composites, which is believed due to the smaller size of CB ($\sim$30 nm) and its round geometry, it can fill up the micro-gaps and micro-pores between GNP platelets, thus providing additional conducting paths. However, upon further increase of CB to 30 wt%, the electrical conductivity is reduced to 13 S cm^{-1}. This interesting phenomenon is based on the fact that the intrinsic electrical conductivity of CB is much lower than that of GNP. The addition of too much CB disrupts the formation of GNP networks which subsequently lowers the overall electrical conductivity of the resulting nanocomposites [39].

Fig. 8 describes the flexural properties of these hybridized nanocomposites. It is noted that both the flexural strength and flexural modulus are not affected much by the addition of CB if the weight ratio between CB and GNP is not larger than 1:2. Huge decrease in the flexural properties is then observed for the PPS/CB/GNP hybrid nanocomposite with 30 wt% CB. Reduction in the flexural properties for this hybridized sample is also believed due to the disruption of GNP network formation by the excess of CB, which fundamentally changes the fracture behavior of the

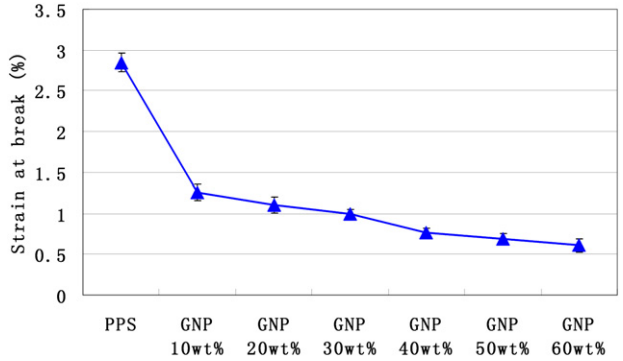

Fig. 4. Strain at break of PPS/GNP nanocomposites made by SSBM and compression molding.

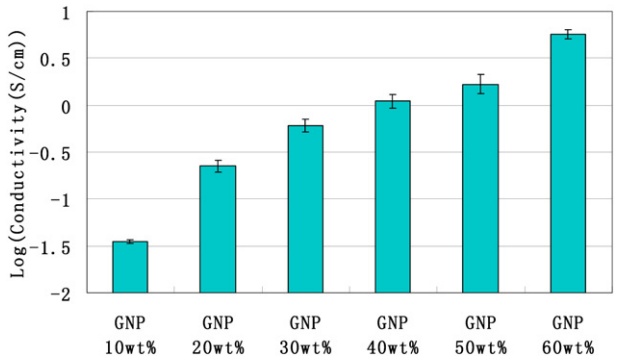

Fig. 6. In-plane electrical conductivity of PPS/GNP nanocomposites made by SSBM and compression molding.

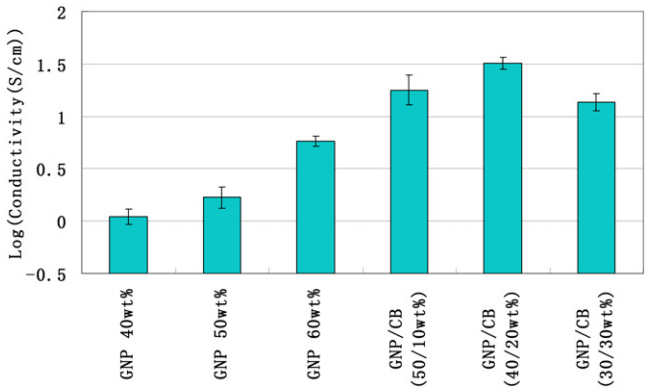

Fig. 7. In-plane electrical conductivity of PPS/CB/GNP hybrid nanocomposites made by SSBM and compression molding.

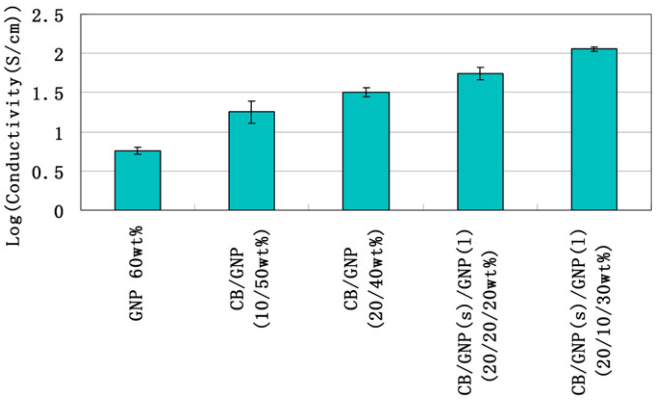

Fig. 9. Synergistic effects on electrical conductivity of combining small GNP platelets with large ones.

nanocomposite. To sum up, the combination of GNP with a proper amount of CB could provide a positive synergistic in improving the electrical conductivity of the resulting nanocomposites while maintaining their flexural strength.

3.3. Synergistic effect in combination of small and large GNP platelets

As discussed in the previous section, the electrical conductivity is substantially improved in the PPS/CB/GNP hybridized nanocomposites. However, the best conductivity got so far ($\sim$32 S cm^{-1}) still does not meet the DOE target. In this case, the GNP size effect was taken into consideration. Based on a previous research, it is known that smaller GNP platelets in the polymer matrix offer better mechanical properties while larger ones contribute to lower percolation threshold or higher electrical conductivity [40]. Combination of smaller GNP platelets with larger ones was then investigated for a positive synergistic effect. Importantly, the size of GNP platelets can be easily controlled by the SSBM time. Take the composition of PPS/CB/GNP(s)/GNP(l) (40:20:20:20 wt%) for example, GNP(s) stands for the small GNP particles which are SSBM processed with PPS and CB for a total of 200 min. The final diameter of this GNP is less than 5 μm as described in the Experimental section. GNP(l) represents larger GNP platelets which are SSBM processed only for 30 min. Their final size is maintained at around 20 μm. Particularly, this portion of GNP is added when the mixture of PPS, CB and GNP(s) is ball milled for 170 min.

The synergistic effect of combining small GNP platelets with larger ones on the electrical and mechanical properties is shown in Figs. 9 and 10 respectively. From Fig. 9, it is clearly seen that the electrical conductivity is tremendously enhanced with the increasing fraction of large GNP platelets (GNP(l)). At the sample composition of HDPE/CB/GNP(s)/GNP(l) (40:20:10:30 wt%), where the total filler loading is still kept at 60 wt%, the in-plane conductivity reaches 114 S cm^{-1}, which has already exceeded the DOE target. Higher electrical conductivity in the nanocomposites with large GNP platelets can be attributed to the fact that the aspect ratio of large GNP platelets is much higher, which makes them interconnect with each other much easier in forming conductive networks in the polymer matrix. And based on the results of the flexural properties displayed in Fig. 10, the flexural strength drops a little as expected in the nanocomposite with 30 wt% GNP(l), but it remains as high as 50 MPa which is twice as much as the DOE target (>25 MPa). Therefore, we may conclude that by properly controlling the amount of large GNP platelets added, both the electrical and the mechanical properties of the resulting nanocomposite can successfully meet the DOE requirements for bipolar plates.

3.4. Fabricating GNP papers and PPS impregnated GNP papers

Based on the results above, the GNP based PPS nanocomposites made by SSBM and compression molding have met the DOE targets for bipolar plates. Here, I propose a novel technique of embedding GNP papers into PPS/GNP nanocomposites which is capable of further enhancing various properties of the resulting GNP based bipolar plates. GNP papers were fabricated by a vacuum filtration method. First of all, GNP-15 nanoplatelets were dispersed in water with the help of polyethylenimine (PEI). The weight ratio between

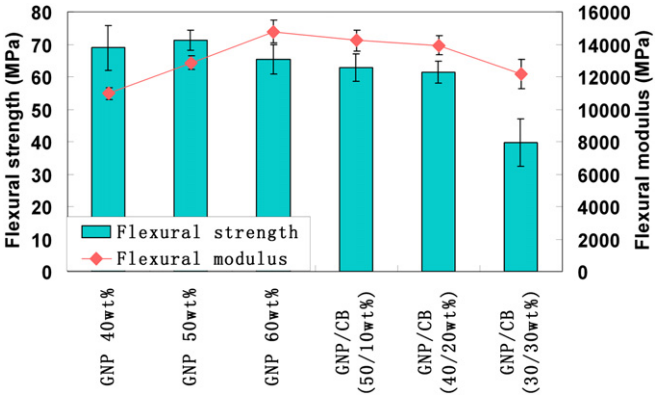

Fig. 8. Flexural properties of PPS/CB/GNP hybrid nanocomposites made by SSBM and compression molding.

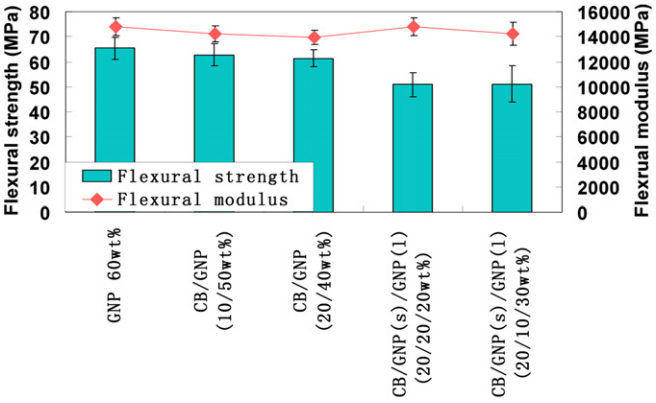

Fig. 10. Synergistic effects on flexural properties of combining small GNP platelets with large ones.

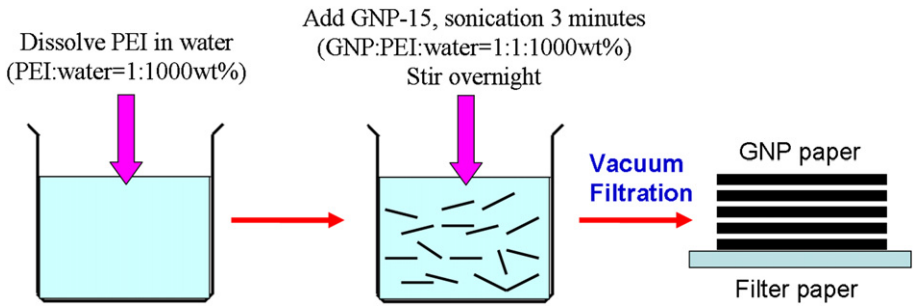

Fig. 11. The procedure of making GNP papers.

GNP-15, PEI and water is 1:1:1000. Ultra-sonication at 100 W was applied for 3 min to break down GNP aggregates and to ensure a better GNP dispersion. Then the GNP suspension was stirred at room temperature for 24 h before it was filtrated with a glass micro-fiber filter paper under vacuum. This GNP filtration procedure is schematically shown in Fig. 11.

The filtered GNP with the filter paper was dried at 100 °C overnight to remove any residual moisture. Due to the hydrophobicity of GNP nanoplatelets, it was very easy to peel the GNP layer off from the hydrophilic glass fiber filter paper. Then the GNP paper was further annealed at 340 °C for 1 h to get rid of the remaining PEI. Fig. 12 shows the morphology of a GNP paper. From the image (a), it is seen the GNP paper made by the vacuum filtration is robust and has some mechanical flexibility. Image (b) shows the cross-section morphology of the paper, from which we can see that GNP platelets exhibit a very good alignment, which provides the mechanical strength to the GNP paper and also ensures excellent in-plane electrical conductivity (>1300 S cm^{-1}) and thermal conductivity (>300 W $(mK)^{-1}$). By increasing the magnification, image (c) reveals the porous nature of the GNP paper, which offers the possibility for the impregnation of polymers into these pores.

To ensure a good adhesion between the GNP papers and the PPS nanocomposites where they are embedded into, GNP papers should be firstly saturated with the host polymer (PPS). In this study, the incorporation of PPS into the GNP papers was achieved by a novel co-filtration technique. First of all, the as-received PPS powder was ball milled for 10 h to reduce its size to around 20–30 μm. The morphology of as-received PPS and the powder after ball milling is shown in Fig. 13.

Then the ball milled PPS powder was dispersed into the PEI/water solution. The weight ratio between PPS, PEI and water is 1:2:1000. Sonication at 100 W was applied for 5 min to break down

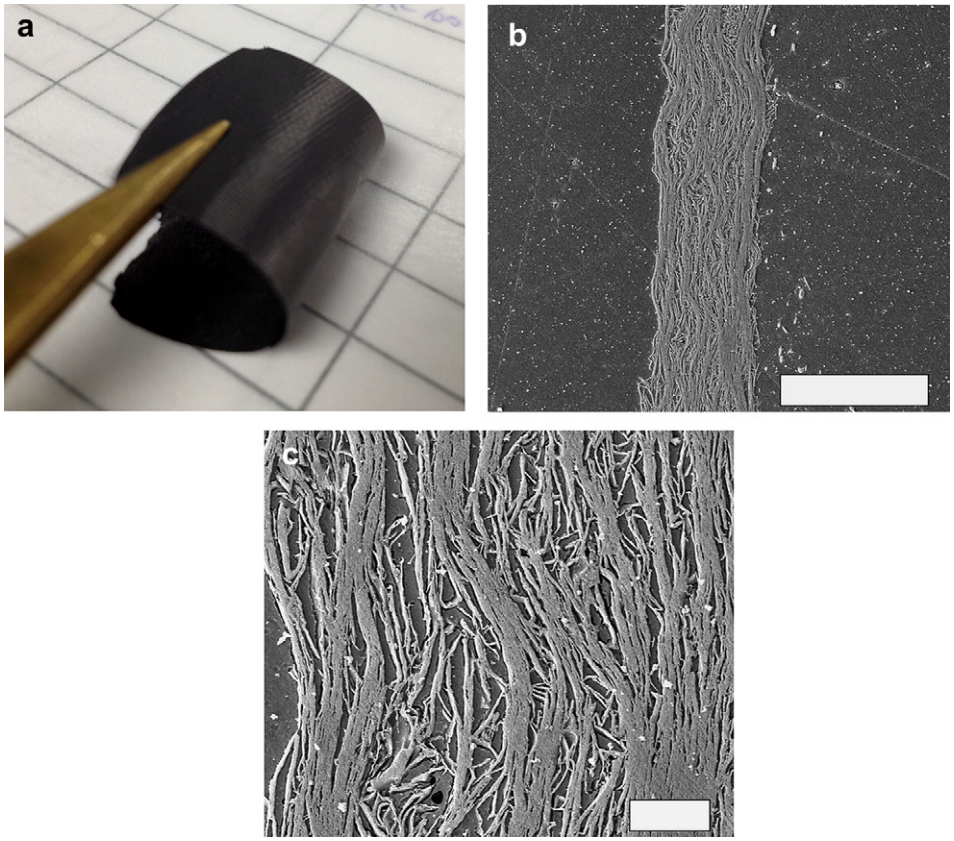

Fig. 12. (a) A mechanically flexible GNP paper made by vacuum filtration; (b) SEM morphology of cross-section of the GNP paper (scale bar 100 μm); (c) enlarged cross-section morphology (scale bar 10 μm).

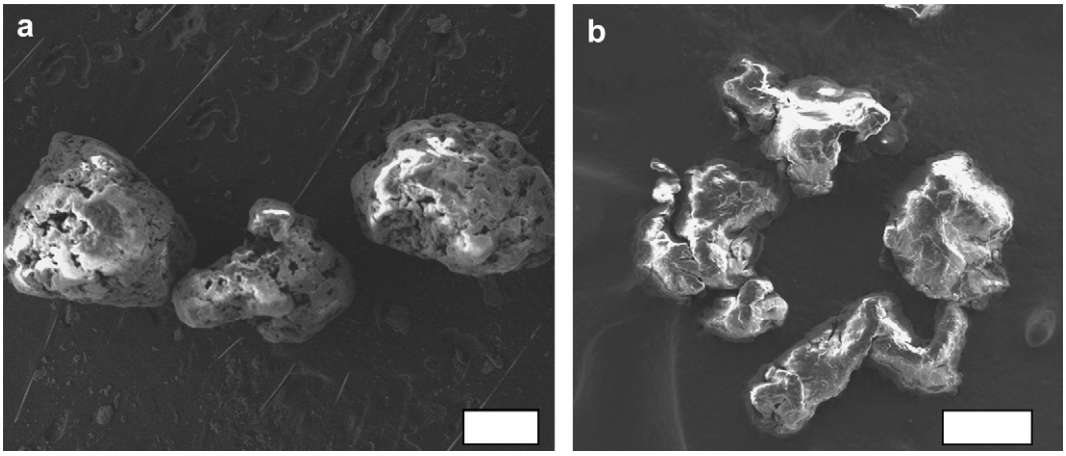

Fig. 13. The morphology of (a) as-received PPS powder (scale bar 300 μm) and (b) the PPS powder after 10 h ball milling (scale bar 30 μm).

any powder aggregates and also for a better PPS dispersion. Then GNP-15 was added into the suspension, another 3 min sonication (100 W) was used under the constant stirring. The weight ratio between all the components was kept as 1:1:2:1000 (GNP:PPS:PEI:water), which makes the PPS content in the resulting PPS impregnated GNP paper to be 50 wt%. The suspension was kept stirring for 24 h before the same vacuum filtration step was applied to filter the GNP with PPS. The resulting GNP paper which contains PPS powder was dried at 100 °C overnight to remove any residual moisture and then the GNP layer was peeled off from the filter paper. It was found that this kind of GNP paper is still self-standing and mechanically robust. The cross-section morphology of the GNP paper is shown in Fig. 14, from which we can clearly see that PPS powders are embedded in the paper.

To fully melt these trapped PPS powders for a better connection and adhesion between GNP platelets and PPS, the GNP paper was firstly annealed at 340 °C in furnace to get rid of excessive PEI and then hot pressed at 325 °C for 5 min under 10 MPa pressure. The cross-section morphology of a hot pressed GNP paper with PPS is then displayed in Fig. 15. According to this figure, it is seen that the GNP paper is fully wetted and covered by the polymer and no platelet morphology can be detected, which suggests the adhesion between PPS and GNP is excellent. The procedure of fabricating PPS impregnated GNP paper through the co-filtration method is then schematically illustrated in Fig. 16.

The thickness of the resulting PPS impregnated GNP paper is around 80 μm and its electrical conductivity was found to be as high as 700 S cm^{-1} even with 50 wt% PPS. This conductive value at 50 wt% GNP loading is much higher than the PPS/GNP nanocomposite made from SSBM and compression molding ($\sim$1.7 S cm^{-1}) as described in Section 3.1. The superb electrical conductivity of the PPS impregnated GNP paper is mainly due to the continuous conductive networks present in the paper which is pre-formed in the GNP paper-making process. Furthermore, the gas (oxygen) permeability of this GNP paper is as low as 2.1×10^{-10} cm^3 $(cm^2\ s)^{-1}$ due to the excellent gas barrier properties of GNP nanoplatelets and their good alignment in the paper.

3.5. Embedding GNP papers into PPS nanocomposites for enhanced electrical and mechanical properties

Because of the excellent electrical conductivity and extremely low gas permeability of the PPS impregnated GNP paper as explored above, it is thus considered as an ideal supplement to be embedded into PPS nanocomposites to further enhance their various properties. The procedure of embedding a PPS impregnated GNP paper into the PPS nanocomposite is schematically shown in Fig. 17. Here PPS/CB/GNP(s)/GNP(l) (40:20:10:30 wt%) powder mixture made from SSBM is used as the host nanocomposite. Of

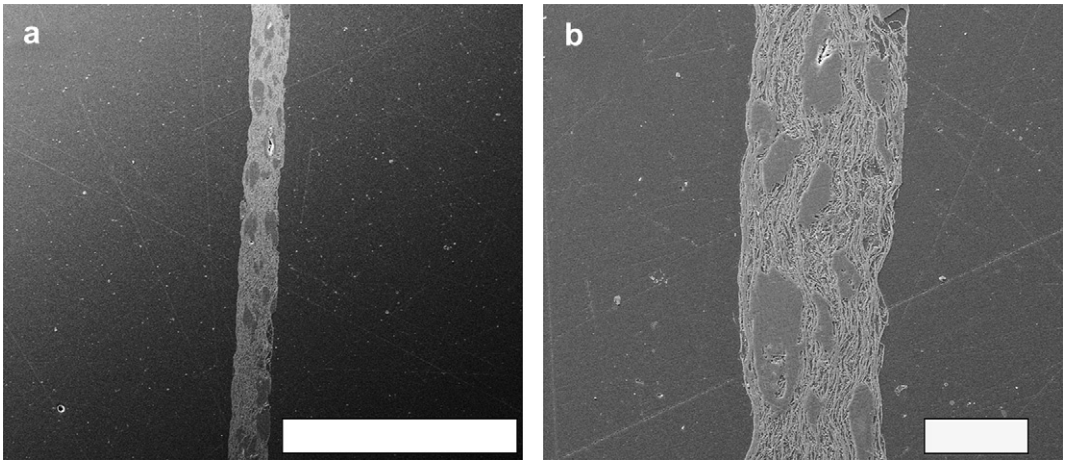

Fig. 14. SEM images show the cross-section morphology of a PPS powder impregnated GNP paper, PPS content: 50 wt% (a) scale bar 1 mm; (b) scale bar 100 μm.

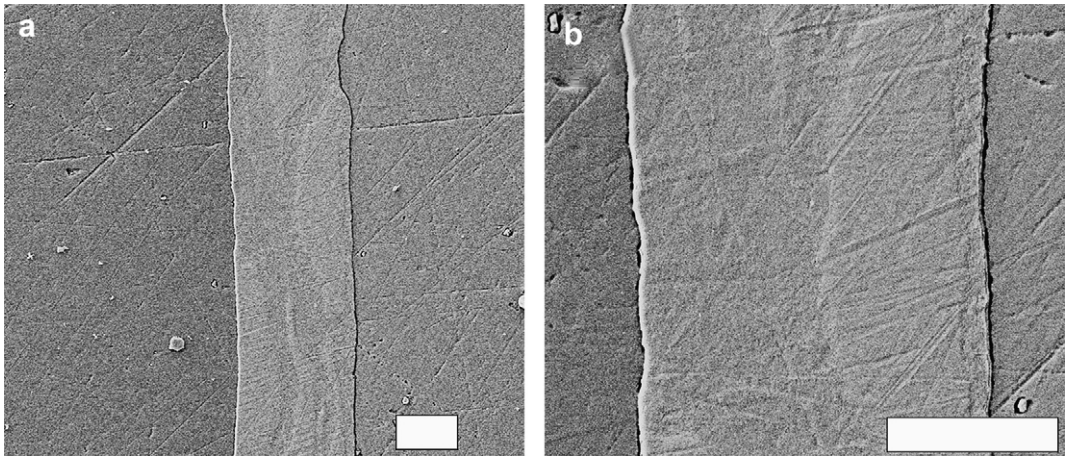

Fig. 15. SEM images show the cross-section morphology of a PPS impregnated GNP paper after hot compression, PPS content: 50 wt% (a) scale bar 30 μm; (b) scale bar 30 μm.

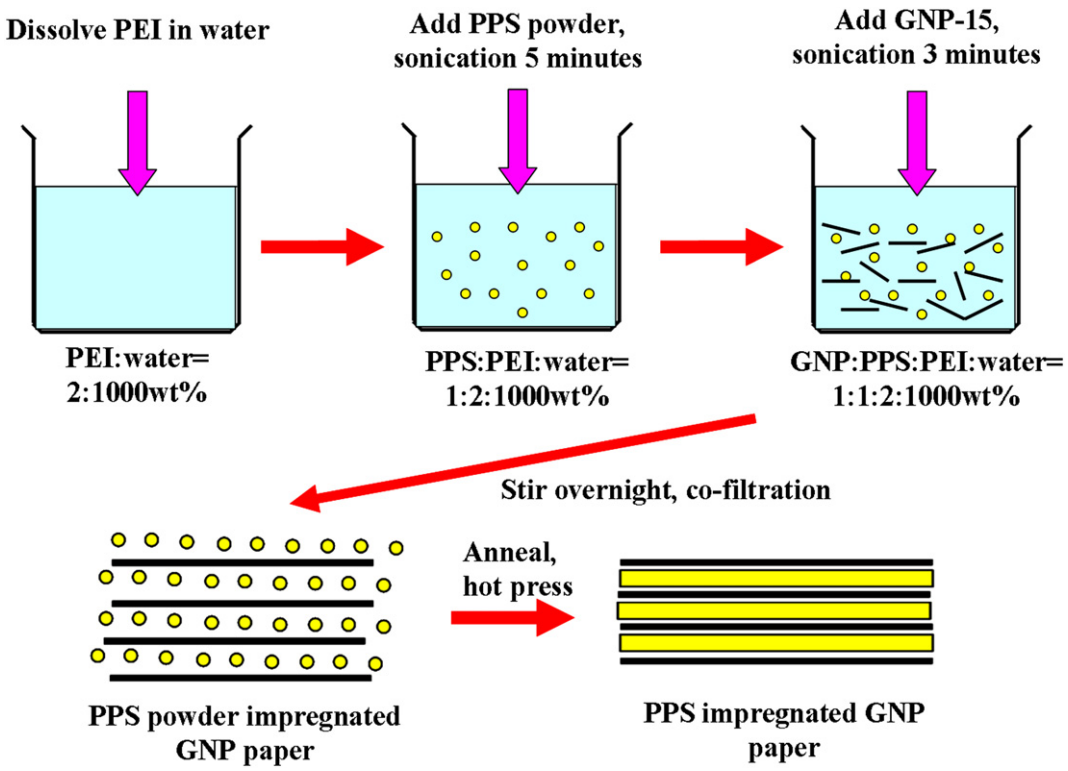

Fig. 16. The procedure of applying a co-filtration technique to fabricate PPS impregnated GNP papers.

course, the number of the GNP paper embedded could be one, two, and more as required.

The in-plane electrical conductivity of the PPS/CB/GNP(s)/GNP(l) (40:20:10:30 wt%) nanocomposites with zero, one, and two PPS impregnated GNP papers inside is shown in Fig. 18, from which it is clearly seen that the in-plane electrical conductivity is significantly enhanced by embedding GNP papers into the host nanocomposite. Moreover, the conductivity is continuously improving as the number of GNP paper embedded increases. The enhancement in conductivity can be attributed to the high electrical conductivity of PPS impregnated GNP papers ($\sim$700 S cm^{-1}).

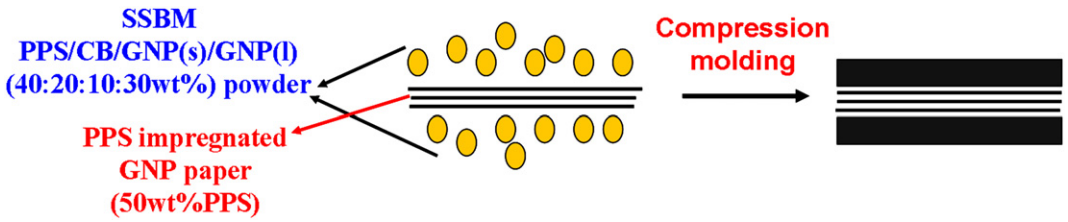

Fig. 17. The procedure of embedding a PPS impregnated GNP paper into a PPS/CB/GNP hybridized nanocomposite.

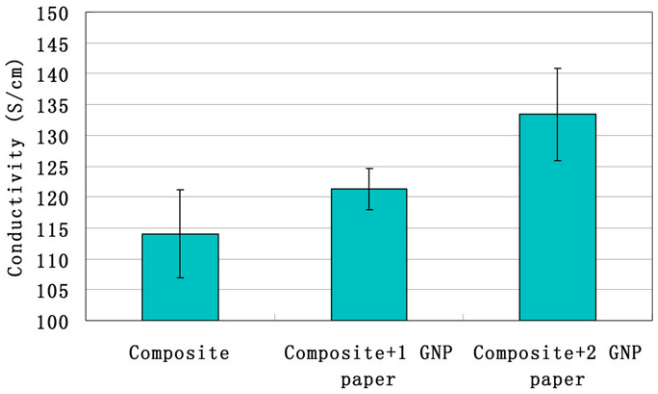

Fig. 18. In-plane electrical conductivity of PPS/CB/GNP(s)/GNP(l) (40:20:10:30 wt%) nanocomposites with zero, one, and two PPS impregnated GNP papers (PPS: 50 wt%).

A model is proposed here to predict the resulting in-plane electrical conductivity of the laminated PPS nanocomposites with GNP papers. That is, if the connection between the GNP paper and the host composite is perfect, they can be considered as two conductors connecting in parallel to each other. So the conductivity of the resulting laminated nanocomposite and the conductivity of each component should have this relationship:

$$S \times t = S_1 \times t_1 + S_2 \times t_2 \quad (2)$$

where S is the conductivity of the laminated nanocomposite; t is its thickness (~3.3 mm); S_1 is the conductivity of the PPS impregnated GNP paper (~700 S cm^{-1}), t_1 is its thickness (~80 μm for one GNP paper); S_2 is the conductivity of the host nanocomposite (~114 S cm^{-1}, as shown in Fig. 18), and $t_2 = t - t_1$.

The experimental data and the conductivity calculated by this model for the laminated nanocomposites with one and two PPS impregnated GNP papers are presented in Fig. 19. From this figure, it is noted that the experimental data is close to the theoretical value which suggests the connection between the GNP paper and the host composite is good although not perfect. Good connection and adhesion come from the fact that the GNP paper is firstly saturated with the host polymer, PPS, before it is embedded into the nanocomposite.

The flexural properties of these laminated nanocomposites are shown in Fig. 20. It is noticed that the flexural strength is enhanced by 20% from 50 MPa to 60 MPa as two PPS impregnated GNP papers are embedded. Higher flexural strength in laminated PPS nanocomposites further confirms the adhesion between the GNP papers and the host nanocomposite is good. Delamination did not occur during the mechanical test, which would otherwise be the major

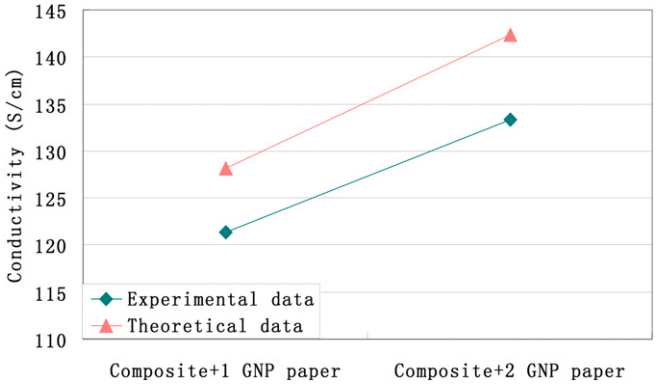

Fig. 19. Experimental and theoretical in-plane electrical conductivity of PPS/CB/GNP(s)/GNP(l) (40:20:10:30 wt%) nanocomposites with one and two PPS impregnated GNP papers (PPS: 50 wt%).

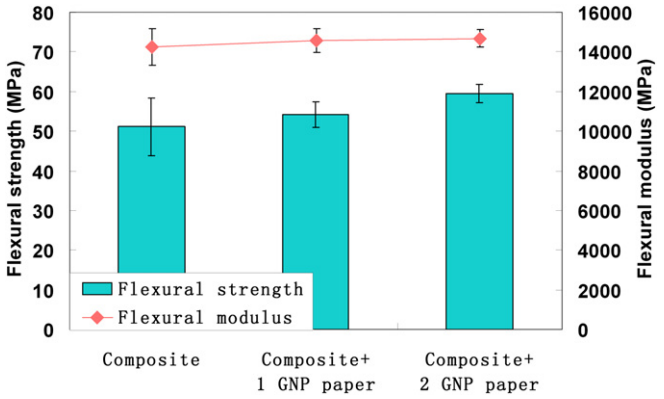

Fig. 20. Flexural properties of PPS/CB/GNP(s)/GNP(l) (40:20:10:30 wt%) nanocomposites with zero, one, and two PPS impregnated GNP papers (PPS: 50 wt%).

reason for the reduction of mechanical strength in laminated composites [41]. In this case, these embedded GNP papers serves as better stress transfer media to resist the shearing and bending force because of their integrity and robustness, which consequently boost the flexural strength of the resulting PPS/GNP nanocomposites.

Although the gas permeability of the nanocomposite with GNP papers has not been tested, it is believed that it should be further reduced based on the extremely low gas permeability of the PPS impregnated GNP paper inside.

4. Conclusion

This study has explored the potential of using PPS/GNP nanocomposites as novel polymeric bipolar plates in fuel cells. PPS/GNP nanocomposites were fabricated by the SSBM and compression molding process and the effectiveness of GNP platelets in enhancing the mechanical properties and lowering the gas permeability of the resulting nanocomposites was investigated.

To increase the electrical conductivity for the DOE target, a synergistic effect between GNP and CB on the electrical conductivity was discussed. It was found that the binary blends of GNP with CB result in a better enhancement in electrical conductivity while maintaining the mechanical properties of the hybridized nanocomposites. Meanwhile, the combination of smaller GNP platelets with larger ones was discovered to be another crucial parameter in determining the various properties of the resulting nanocomposites. These synergistic effects have offered a useful insight into the processing of polymeric bipolar plates with tailored properties to meet the stringent requirements. Furthermore, the process of embedding PPS impregnated GNP papers into PPS nanocomposites has been developed, which is capable of further improving electrical, mechanical and gas barrier properties.

To sum up, this study has provided two scientific approaches (synergistic effects and embedding GNP papers) to optimize the various properties of PPS/GNP nanocomposites for their application in bipolar plates. Low filler loading, low material cost and easy fabrication of these PPS/GNP bipolar plates will allow lighter weight and lower cost of PEM fuel cells with enhanced performance which is particularly suited for automotive applications.

Acknowledgment

This research was supported under Army Research Office Grant No. W91INF-09-1-0451, “Center for Alternative Energy Storage Research and Technology”.

References

[1] O. Savadogo, ChemInform 29 (1998) 47–66.
[2] E. Petrach, I. Abu-Isa, W. Xia, Journal of Composite Materials 44 (2010) 1665–1676.
[3] V. Mehta, J.S. Cooper, Journal of Power Sources 114 (2003) 32–53.
[4] D.P. Davies, P.L. Adcock, M. Turpin, S.J. Rowen, Journal of Applied Electrochemistry 30 (2000) 101–105.
[5] S.-H. Liao, C.-C. Weng, C.-Y. Yen, M.-C. Hsiao, C.-C.M. Ma, M.-C. Tsai, A. Su, M.-Y. Yen, Y.-F. Lin, P.-L. Liu, Journal of Power Sources 195 (2010) 263–270.
[6] B. Cunningham, D.G. Baird, Journal of Materials Chemistry 16 (2006) 4385–4388.
[7] B.K. Kakati, V.K. Yamsani, K.S. Dhathathreyan, D. Sathiyamoorthy, A. Verma, Carbon 47 (2009) 2413–2418.
[8] C.E. Borroni-Bird, Journal of Power Sources 61 (1996) 33–48.
[9] E.A. Cho, U.S. Jeon, H.Y. Ha, S.A. Hong, I.H. Oh, Journal of Power Sources 125 (2004) 178–182.
[10] H. Wang, J.A. Turner, Fuel Cells 10 (2010) 510–519.
[11] R.A. Antunes, M.C.L. Oliveira, G. Ett, V. Ett, International Journal of Hydrogen Energy 35 (2010) 3632–3647.
[12] S. Yoshiyuki, Surface and Coatings Technology 202 (2007) 1252–1255.
[13] Y.-M. Lee, S.-J. Lee, C.-Y. Lee, P.-H. Lai, Journal of Fuel Cell Science and Technology 7 (2010) Article Number: 031016.
[14] S.K. Kamarudin, W.R.W. Daud, A. Md.Som, M.S. Takriff, A.W. Mohammad, Journal of Power Sources 157 (2006) 641–649.
[15] R.B. Mathur, S.R. Dhakate, D.K. Gupta, T.L. Dhami, R.K. Aggarwal, Journal of Materials Processing Technology 203 (2008) 184–192.
[16] S. Radhakrishnan, B.T.S. Ramanujam, A. Adhikari, S. Sivaram, Journal of Power Sources 163 (2007) 702–707.
[17] C. Hui, H.-B. Liu, J.-X. Li, Y. Li, Y.-D. He, Journal of Composite Materials (2009).
[18] S.-H. Liao, C.-H. Hung, C.-C.M. Ma, C.-Y. Yen, Y.-F. Lin, C.-C. Weng, Journal of Power Sources 176 (2008) 175–182.
[19] R.A. Antunes, M.C.L. de Oliveira, G. Ett, V. Ett, Journal of Power Sources 196 (2011) 2945–2961.
[20] S. Biswas, H. Fukushima, L.T. Drzal, Composites Part A: Applied Science and Manufacturing 42 (2011) 371–375.
[21] H. Fukushima, L. Drzal, B. Rook, M. Rich, Journal of Thermal Analysis and Calorimetry 85 (2006) 235–238.
[22] L.T.D. Hiroyuki Fukushima, in: ANTEC-Society of Plastics Engineers, 2003, pp. 2230–2234.
[23] H.F. Kyriaki Kalaitzidou, Lawrence T. Drzal, Carbon 45 (2007) 1446–1452.
[24] L.-g. Xia, A.-j. Li, W.-q. Wang, Q. Yin, H. Lin, Y.-b. Zhao, Journal of Power Sources 178 (2008) 363–367.
[25] X. Jiang, L.T. Drzal, Journal of Applied Polymer Science 124 (2012) 525–535.
[26] M. Endo, H. Muramatsu, T. Hayashi, Y.A. Kim, M. Terrones, M.S. Dresselhaus, Nature 433 (2005) 476.
[27] Y.A. Kim, H. Muramatsu, T. Hayashi, M. Endo, M. Terrones, M.S. Dresselhaus, Chemical Vapor Deposition 12 (2006) 327–330.
[28] J. Gou, Polymer International 55 (2006) 1283–1288.
[29] X. Yan, Z. Tai, J. Chen, Q. Xue, Nanoscale 3, 212–216.
[30] H. Lu, Y. Liu, J. Gou, J. Leng, S. Du, International Journal of Smart and Nano Materials 1, 2–12.
[31] H. Chen, M.B. Müller, K.J. Gilmore, G.G. Wallace, D. Li, Advanced Materials 20 (2008) 3557–3561.
[32] O.C. Compton, D.A. Dikin, K.W. Putz, L.C. Brinson, S.T. Nguyen, Advanced Materials 22, 892–896.
[33] http://www.buckypaper.com/.
[34] O.C. Compton, S.T. Nguyen, Small 6, 711–723.
[35] H. Wu, Michigan State University, PhD thesis, 2011.
[36] GNP is an exfoliated graphene nanoplatelet material obtained from XG Sciences, Inc., East Lansing, MI (www.xgsciences.com).
[37] C. Du, P. Ming, M. Hou, J. Fu, Q. Shen, D. Liang, Y. Fu, X. Luo, Z. Shao, B. Yi, Journal of Power Sources 195 (2010) 794–800.
[38] X. Jiang, L.T. Drzal, in: 11th Annual SPE ACCE Conference Troy, Michigan, 2011.
[39] S.R. Dhakate, S. Sharma, M. Borah, R.B. Mathur, T.L. Dhami, Energy & Fuels 22 (2008) 3329–3334.
[40] X. Jiang, L.T. Drzal, in: 41st International SAMPE Technical Conference (ISTC), Wichita, Kansas, 2009.
[41] W.J. Cantwell, J. Morton, The Journal of Strain Analysis for Engineering Design 27 (1992) 29–42.